Calculation of Capture Point Considering the Existence of Collision

Huawei Wang, Chenglong Fu

Abstract: Capture theory is important not only for humanoid robot but also for amputees to adapt to more complex situation. This paper calculated the capture point considering the existence of collision between ground and leg. Collision could reduce the velocity of CoM which is helpful for human to be captured. On the basic kinetics of Three-Dimensional Linear Inverted Pendulum Model (3D-LIPM), three collision models are proposed here. Even though we could not prove which collision model could describe the collision process best, the capture point results of all the collision models could make up the conservative property of 3D-LIPM without collision.

1. Introduction

Push recovery ability has been received much attention in recent years because it is essential for biped robot to work in non-lab environment. This ability could prevent biped robot from falling down when facing some perturbations or even big collision. Several strategies, including ankle strategy, hip strategy, step strategy, are generated to achieve the push recovery ability in past decades. Among these strategies, capture theory is the most completed and has been proved very effective in biped robot [1, 2].

Even though capture theory based on the 3D-LIPM has a relatively complete and inspiring result, it is conservative because of strict hypothesis. One strict hypothesis is that the collision between swing leg and ground was not considered. Indeed, this hypothesis could keep the orbital energy of 3D-LIPM constantly before and after legs shift and make the capture point calculation into a wonderful linear formula [3]. However, the collision between swing leg and ground is helpful to human reaching a capture state, since it reduces the orbital energy during legs shifting. Therefore, in this paper, we primarily interested in the influence of capture point calculating if the collision is taken into consideration. In human’s motion, this collision means

heel-strike, which is a very complex process [4]. It is impossible to fully simulate this process. In this case, we chose three ideal collision models to represent the heel-strike process.

The structure of this paper is as follow. Section 2 is used to apply collision models into 3D-LIPM with point foot. The extended applications to 3D-LIPM with finite foot as well as reaction mass are mentioned at Section 3. Section 4 compares the results of capture point in different models. Discussion is present in Section 5.

2. 3D-LIPM and collision models

This section calculates analytical motion functions of capture point of 3D-LIPM when applied different collision models. To begin with, we choose 3D-LIPM with point foot as the model base. In next section, these analytical results will be explored to 3D-LIPM with finite-size foot as well as 3D-LIPM with finite-size foot and reaction mass.

2.1 The kinetics of 3D-LIPM

3D-LIPM with point foot is the simplest model of 3D-IPM that assumes the point mass is kept in a horizontal plane. This hypothesis brings an important superiority that the kinetics of 3D-LIPM in x-y plane becomes a spring-mass system. In this case, the kinetics of 3D-LIPM is linear and the x, y orientation is decoupled and could be calculated separately. In the first step, kinetics of 3D-LIPM before collision is analyzed as follow.

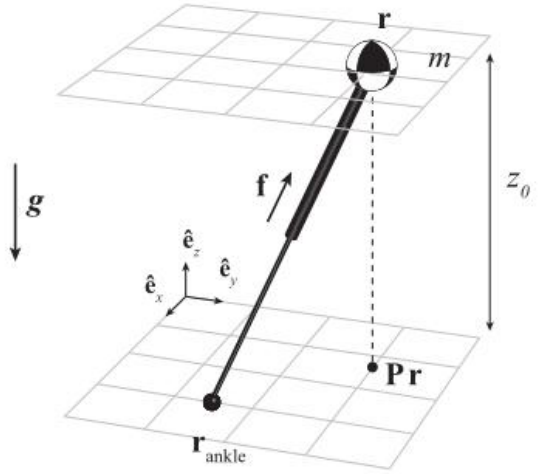

Fig 1 3D-LIPM with point foot [2].

From the definition of 3D-LIPM with point foot, we could get the motion of the point mass is

$$\ddot{r}' = P \cdot r' - r_{ankle}' \tag{2.1}$$

Where: $P = \begin{bmatrix} 1 & 0 & 0 \\ 0 & 1 & 0 \\ 0 & 0 & 0 \end{bmatrix}$; $r_{ankle}' = \frac{r_{ankle}}{z_0}$ is the dimensionless point foot location; $r' = \frac{r}{z_0}$ is the dimensionless point mass location; $\ddot{r}' = \frac{\ddot{r}}{g}$ is the dimensionless acceleration of the point mass [2].

Solving the equation 2.1, the displacement and velocity of CoM could be got as follow,

$$r'(\Delta t') = C_1 \cdot e^{\Delta t'} + C_2 \cdot e^{-\Delta t'} + r_{ankle}' \tag{2.2}$$

$$\dot{r}'(\Delta t') = C_1 \cdot e^{\Delta t'} - C_2 \cdot e^{-\Delta t'} \tag{2.3}$$

where: $C_1 = \frac{(r'(0) - r_{ankle}') + \dot{r}'(0)}{2}$

$$C_2 = \frac{(r'(0) - r_{ankle}') - \dot{r}'(0)}{2}$$

2.2 Capture point calculating of different collision models

Based on the above kinetics function of 3D-LIPM with point foot, the capture point calculation is determined by the collision models. Firstly, the instantaneous capture point is calculated, and then lead to the time varying capture point function. In order

to clearly show the velocity changes during collision, the schematics in this section are all planar graphs. Because 3D-LIPM and collision models are x, y direction decoupled, the calculations are in three dimensional. Here, we also define the distance between instantaneous capture point and CoM as x'. With this definition, the calculation function of instantaneous capture point could be clearly expressed.

2.2.1. No collision

The hypothesis of no collision is that legs shift instantaneously, and no velocity changes during this period. Velocities of CoM before and after leg shift are shown in Fig 2.

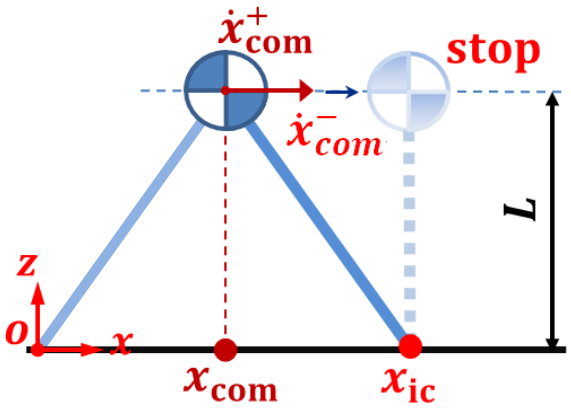

Fig 2 the change of velocities when legs shift without collision

Because there is no energy lost between leg shifts, the dimensionless orbital energies keeps in constant [3, 5, 6]. The instantaneous capture point of this model is as follow,

$$x' = \dot{r}' \tag{2.4}$$

where， $x' = r_{ic}' - r'$

Combine with equation 2.2 and 2.3, the time variable function of capture point could be calculated as follow:

$$r_{ic}'(\Delta t') = (r'(0) + \dot{r}'(0) - r_{ankle}') \cdot e^{\Delta t'} + r_{ankle}' \tag{2.5}$$

2.2.2. Collision model 1

The hypotheses of collision model 1 are as follow, and the change of velocities before and after collision is shown in Fig 3.

1. The velocities of CoM before and after collision only exist in the horizontal plane.
2. The collision is ideal and happens instantaneously.
3. During collision and after the legs shifting, the length of trailing leg keeps constant.

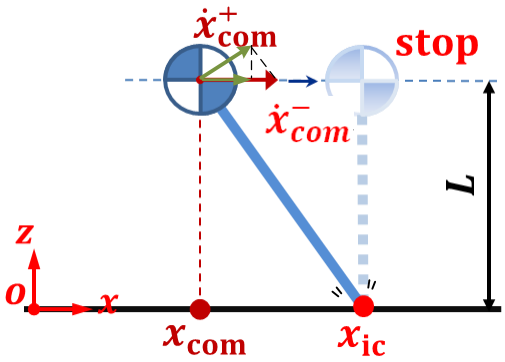

Fig 3 Velocities change when legs shifting of collision model 1

According to the hypotheses and velocities changes before and after collision, the instantaneous capture point of this model is calculating as follow,

$$x' = \frac{\dot{r}'}{1+x'^2} \tag{2.6}$$

where， $x' = r_{ic}' - r'$

Solving equation 2.8, the time varying capture point location is as follow,

$$r_{ic}'(\Delta t') = Pr'(\Delta t') + \sqrt[3]{\frac{\dot{r}'(\Delta t')}{2} - \sqrt{\left(\frac{\dot{r}'(\Delta t')}{2}\right)^2 + \left(\frac{1}{3}\right)^3}} + \sqrt[3]{\frac{\dot{r}'(\Delta t')}{2} + \sqrt{\left(\frac{\dot{r}'(\Delta t')}{2}\right)^2 + \left(\frac{1}{3}\right)^3}} \tag{2.7}$$

Combine with equation 2.2 and 2.3, the location of time varying capture point could be calculated.

2.2.3. Collision Model 2

Hypotheses:

1. The velocities of CoM before and after collision only exist in the horizontal plane.
2. The collision is ideal and happens instantaneously.
3. During collision, both the leading leg and trailing leg keep in constant length L (L

is the length of original leg).

4. After the collision, the velocity of mass is vertical to the leading leg.

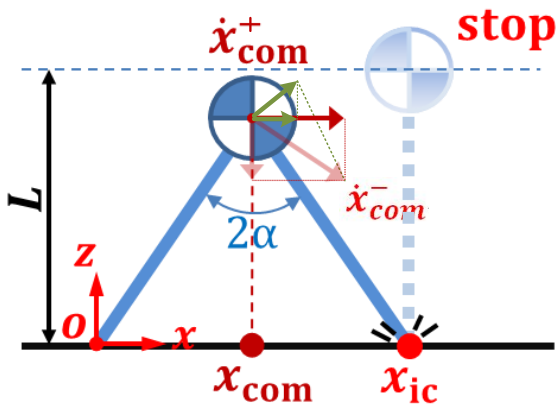

Fig 4 Velocities change when legs shifting of collision model 2

According to the hypotheses and velocities changes before and after collision, the instantaneous capture point of this model is calculating as follow,

$$x' = \left(1 - x'^{2}\right) \cdot \dot{r}' \tag{2.8}$$

where， $x' = r_{ic}' - r'$

Solving equation 2.8, the time varying capture point location is as follow,

$$r_{ic}'(\Delta t') = Pr'(\Delta t') + \frac{-1+\sqrt{1+4\cdot\dot{r}'(\Delta t')^{2}}}{2\cdot\dot{r}'(\Delta t')} \tag{2.9}$$

Combine with equation 2.2 and 2.3, the location of time varying capture point could be calculated.

2.2.4. Collision Model 3:

Hypotheses:

1. The velocities of mass before and after collision only exist in the horizontal plane.
2. The collision is ideal and happens instantaneously.
3. During collision, the mass is still kept in the same horizontal plane.
4. During collision, both the leading leg and trailing leg keep in the same constant length.

5. During the collision, the velocity of mass is vertical to the leading leg.

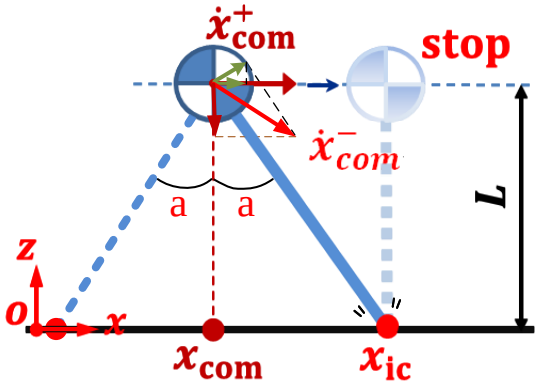

Fig 5 Velocities change when legs shifting of collision model 3

According to the hypotheses and velocities changes before and after collision, the instantaneous capture point of this model is calculating as follow,

$$x' = \frac{1-x'^2}{1+x'^2} \cdot \dot{r}' \tag{2.10}$$

where， $x' = r_{ic}' - r'$

Solving equation 2.10, the time varying capture point location is as follow,

$$r_{ic}'(\Delta t') = Pr'(\Delta t') + \sqrt[3]{-q'(\Delta t') - \sqrt{(q'(\Delta t'))^2 + (p'(\Delta t'))^3}} + \sqrt[3]{-q'(\Delta t') + \sqrt{(q'(\Delta t'))^2 + (p'(\Delta t'))^3}} - \frac{1}{3} \cdot \dot{r}'(\Delta t') \tag{2.11}$$

Where: $q'(\Delta t') = \frac{1}{27} \cdot \dot{r}'(\Delta t')^3 - \frac{1}{6} \cdot \dot{r}'(\Delta t') - \frac{1}{2} \cdot \dot{r}'(\Delta t'),\ p' = \frac{1}{3} - \frac{1}{9} \cdot \dot{r}'\ (\Delta t')^2$

Combine with equation 2.2 and 2.3, the time variable function of capture point could be calculated.

3. Extend to more complex 3D-LIPM models.

In this section, we explored the capture point calculating intro 3D-LIPM with finite-size foot and reaction mass models. For these two models, we still assume that the collision process between leg and ground during legs shift is still the same as above description. Because the equations of instantaneous capture point and time varying capture point are only related on $r'(\Delta t')$ and $\dot{r}'(\Delta t')$, the kinetics of 3D-LIPM with finite-size foot and 3D-LIPM with finite-size foot and reaction mass models should be calculated only.

3.1 3D-LIPM with finite-size foot

3D-LIPM with finite-size foot model is shown in Fig 6.

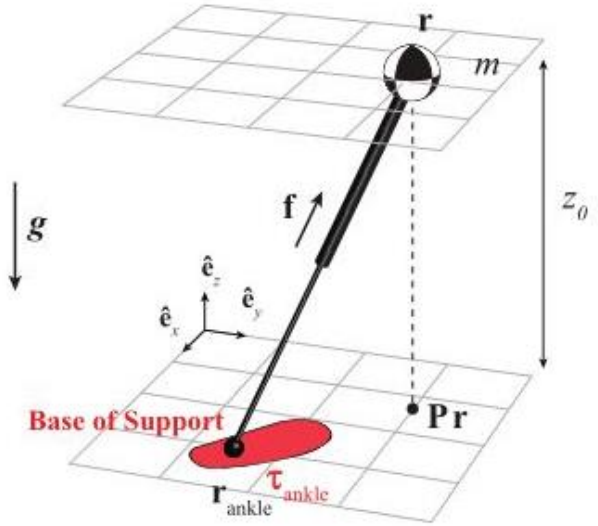

Fig 6 3D-LIPM with finite-size foot [3].

According to Twan's article [3], the kinetics of point mass is

$$\ddot{r}' = P \cdot r' - r_{CoP}' \tag{3.1}$$

Where $\mathrm{r_{CoP}}' = \mathrm{r_{ankle}}' + \Delta \mathrm{r_{CoP}}'$ is the dimensionless position of central of pressure; $\Delta \mathrm{r_{CoP}}' = -\frac{1}{\mathrm{mgz_0}} \begin{pmatrix} \tau_{\mathrm{ankle,y}} \\ -\tau_{\mathrm{ankle,x}} \\ 0 \end{pmatrix}$ is the position deviation between ankle and CoP by applying ankle torque.

$$r'(\Delta t') = C_1 \cdot e^{\Delta t'} + C_2 \cdot e^{-\Delta t'} + r_{CoP}' \tag{3.2}$$

$$\dot{r}'(\Delta t') = C_1 \cdot e^{\Delta t'} - C_2 \cdot e^{-\Delta t'} \tag{3.3}$$

where:

$$C_1 = \frac{(r'(0) - r_{CoP}') + \dot{r}'(0)}{2}$$

$$C_2 = \frac{(r'(0) - r_{CoP}') - \dot{r}'(0)}{2}$$

3.2 3D-LIPM with finite-sized foot and reaction mass

3D-LIPM with finite-sized foot and reaction mass model is shown in Fig 7.

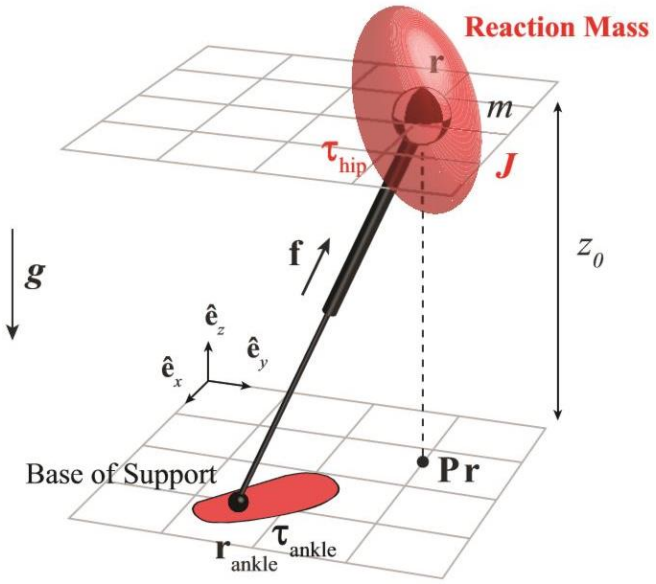

Fig 7 3D-LIPM with finite-sized foot and reaction mass[3]

With the bang-bang torque profiles[3], the motion of this model could be calculated as follow:

$$\ddot{r}' = P \cdot r' - r_{CMP}' \tag{3.4}$$

$$\dot{\omega}' = P \cdot \tau_{hip}' \tag{3.5}$$

Where: $\mathrm{r_{CMP}}' = \mathrm{r_{CoP}}' + \Delta \mathrm{r_{CMP}}'$ is the dimensionless position of central of pressure; $\Delta \mathrm{r_{CMP}}' = \tau_{hip}' \times \hat{e}_z$ is the position deviation between ankle and CoP by applying ankle torque.

$$r'(\Delta t') = C_1 \cdot e^{\Delta t'} + C_2 \cdot e^{-\Delta t'} + r_{CMP}' \tag{3.6}$$

$$\dot{r}'(\Delta t') = C_1 \cdot e^{\Delta t'} - C_2 \cdot e^{-\Delta t'} \tag{3.7}$$

where:

$$C_1 = \frac{(r'(0) - r_{CMP}') + \dot{r}'(0)}{2}$$

$$C_2 = \frac{(r'(0) - r_{CMP}') - \dot{r}'(0)}{2}$$

4. Result

This section compares the capture point results of different collision models. Instantaneous capture point results are compared first, shown in Fig 8. Time varying

capture point results are compared in Fig 9.

In Fig 8, X-axis represents velocity of CoM and Y-axis represents the distance between instantaneous capture point and the location of CoM. Red line is the result of 3D-LIPM without collision. Green line is the result of 3D-LIPM with collision model 1. Blue line is the result of 3D-LIPM with collision model 2. Pink line is the result of 3D-LIPM with collision model 3. The result of 3D-LIPM without collision is linear, which means that the instantaneous capture point will go to infinite distance along with the increase of CoM velocity. However, with the increase of velocity of CoM, the results of 3D-LIPM with collision models approach to a constant value. This means that, collision is helpful for human to get into capture state. A preliminary human push recovery test also indicates that the collision is useful, especially when under large pushes (high CoM velocity).

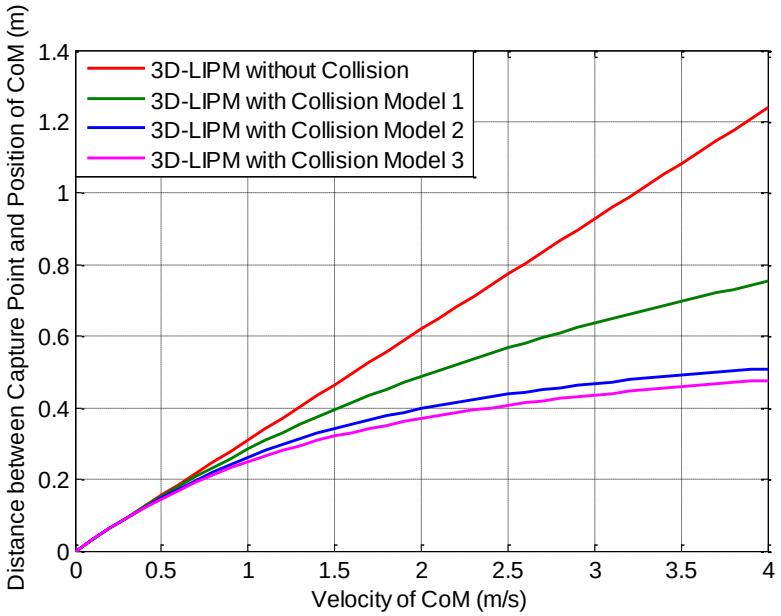

Fig 8 Comparison of instantaneous capture point results of different models. X-axis represents velocity of CoM, and Y-axis represents the distance between instantaneous capture point and the location of CoM. Red line is the result of 3D-LIPM without collision. Green line is the result of 3D-LIPM with collision model 1. Blue line is the result of 3D-LIPM with collision model 2. Pink line is the result of 3D-LIPM with collision model 3.

The initial situation of Fig 9 is as following: the foot location of trailing leg is defined as original point and the CoM is vertically above the original point. The instantaneous capture point of this initial situation is located in origin, which means the initial situation is captured. Instantaneously, the outside perturbation gives the CoM a velocity of 0.6 *m/s*. Then the location of instantaneous capture point begin to change, and the capture point locations of different models are represent in Fig 9 along with different swing leg remain time. In Fig 9, X-axis represents swing leg remaining dimensionless time, and Y-axis represents the location of capture point relative to the origin. When the remaining time is zero, the capture point reduced to instantaneous capture point. Along with the increase of remaining time, the locations of capture points calculating based on different models all increase as an exponential function. This is caused by the kinetics of 3D-LIPM and has no relationship with whether a collision is considered or not.

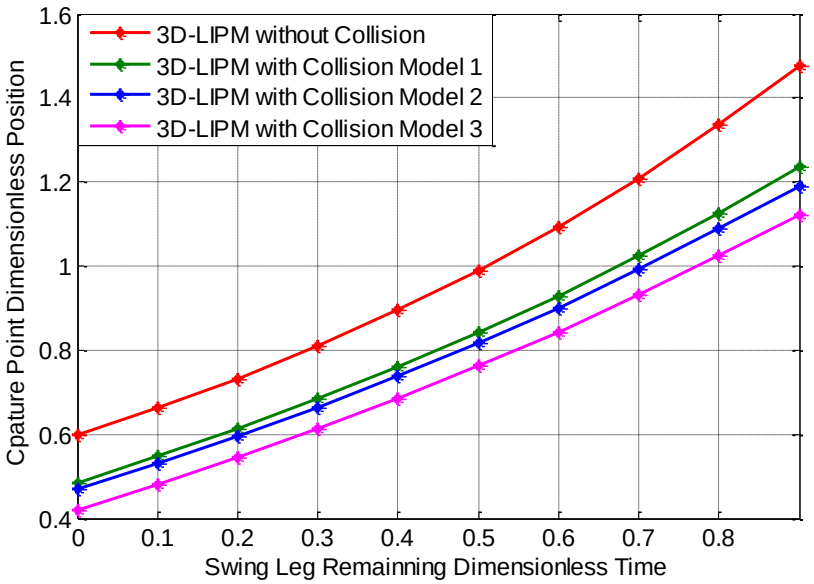

Fig 9 Capture point locations of different models along with different swing leg remaining time. X-axis represents swing leg remaining dimensionless time, and Y-axis represents the location of capture point relative to the origin.

5. Discussion

From the results in section 4, it is clear that adding collision models could partially make up the conservative feature of 3D-LIPM. In human push recovery reactions,

collision always happen during legs shifting. Considering Inverted Pendulum Model (IPM), if the angle between two legs when shifting is ninety degrees, the collision could resist the infinite velocity of CoM which means infinite perturbation. However, in 3D-IPM models, the kinetics of x, y directions are coupled, thus the analytical result of capture point in 3D motion could not achieve. Without analytical results, the capture point could only be calculated by solving complex differential equations as well as equation set, which is time-consuming and not real-time. As the outside perturbation could lead to human and robot quickly falling down, time-consuming means inapplicable.

We have applied the capture point results of collision models into M2V2, which is a wonderful platform established by IHMC to verify the capture theory. However, because push recovery ability also highly related to the planning of swing leg trajectory, push recovery ability of M2V2 did not obviously increase. Currently, we are trying to carry out a rigorous human push recovery experiment to evaluate the collision models.

References:

[1]. Pratt, J., et al. Capture Point: A Step toward Humanoid Push Recovery. 2006: IEEE.

[2]. Jerry Pratt, T.K.T.D., Capturability-Based Analysis and Control of Legged Locomotion, Part 2: Application to M2V2, a Lower Body Humanoid, in The International Journal of Robotics Research. 2012.

[3]. Twan Koolen, T.D.B.J., Capturability-Based Analysis and Control of Legged Locomotion Part1: Theory and Application to simple Gait Models, in The International Journal of Robotics Research. 2011.

[4]. Kuo, A.D., J.M. Donelan and A. Ruina, Energetic consequences of walking like an inverted pendulum: step-to-step transitions. Exercise and sport sciences reviews, 2005. 33(2): p. 88-97.

[5]. Shuuji Kajita, F.K.K.K., The 3D Linear Inverted Pendulum Mode: A simple

modeling for a
biped walking pattern generation, in ICRS. 2001: Hawaii, USA.
[6]. Kajita, S. and K. Tan. Study of dynamic biped locomotion on rugged terrain-derivation and application of the linear inverted pendulum mode. in Robotics and Automation, 1991. Proceedings., 1991 IEEE International Conference on. 1991: IEEE.